Isolation, Optical Properties and Core Structure of a Water-soluble, Phosphine-stabilized $[Au_9]^{3+}$ Cluster

Benjamin S. Gutrath[a,b], Carina Merkens[a], Frank Schiefer[a,b], Ulli Englert[a], Günter Schmid[c], and Ulrich Simon[a,b]

[a] Institute of Inorganic Chemistry, RWTH Aachen University, 52074 Aachen, Germany

[b] JARA – Fundamentals of Future Information Technologies, RWTH Aachen University, 52074 Aachen, Germany

[c] Institute of Inorganic Chemistry, University Duisburg-Essen, 45127 Essen, Germany

Reprint requests to Prof. Dr. Ulrich Simon. Fax: +49 241 80 99003.
E-mail: ulrich.simon@ac.rwth-aachen.de

Dedicated to Professor Heinrich Nöth on the occasion of his 85th birthday

A water-soluble, crystalline Au_9 cluster compound stabilized with sodium (*m*-sulfonatophenyl)diphenylphosphine (TPPMSNa) was obtained during the $NaBH_4$ reduction of $[Au(TPPMSNa)Cl] \cdot H_2O$ in ethanol. Characterization by optical extinction spectroscopy, single-crystal X-ray diffraction in combination with energy dispersive X-ray diffraction led to the preliminary formula $Na_{(8-x)}[Au_9(TPPMS)_8]Cl_{(3-x)} \cdot nH_2O$ ($0 \leq x \leq 3$, $n \approx 16$) with the cluster core in crown conformation. $^{31}P\{^1H\}$ nuclear magnetic resonance spectroscopy revealed one singlet at 57.3 ppm. This is the first example where gold clusters stabilized by TPPMSNa formed crystals which where suitable for core structure determination.

Key words: Cluster Compounds, Gold, Structure Elucidation, Nanotechnology

Introduction

Ligand-stabilized gold nanoparticles (AuNPs) have been the objects of intense studies in nanoscience and -technology for more than two decades due to their unique physical properties, which arise from size quantization effects [1 – 3]. Most recently ultrasmall AuNPs became also of considerable interest in biomedical research, since unexpected cytotoxicity was discovered for water-soluble AuNPs in the size range below 2 nm [4, 5]. These studies revealed that even slight changes in the particle size can have significant influence on the toxicity profile, *e. g.* on the pathway of cell death. Hence, it would be highly desirable to gain control of the particle size of water-soluble AuNPs with atomical precision, as it has been demonstrated for numerous molecular gold clusters, which are only soluble in organic solvents [6].

For the synthesis of molecular gold clusters typically phosphine gold(I) complexes are reduced with boranes or borohydrides in organic solvents [7, 8]. For instance, well-formed crystals of $[Au_9(PPh_3)_8](NO_3)_3$ can be obtained reliably by reducing $[Au(PPh_3)NO_3]$ with $NaBH_4$ in ethanol, followed by purification and crystallization from diluted solutions [9]. The cluster cation $[Au_9(PPh_3)_8]^{3+}$ can be crystallized in two conformations of the gold polyhedron, the so-called crown structure and the butterfly structure [10, 11]. It was found that $[Au_9(PPh_3)_8](NO_3)_3$ in its butterfly conformation shows luminescence in the near infrared (NIR) in the solid state, which is advantageous for biomedical imaging [9].

In order to transform this cluster into a water-soluble derivative we recently performed a two-phase ligand exchange with sodium (*m*-sulfonatophenyl)diphenylphosphine (commonly known as mono-sulfonated triphenylphosphine or as TPPMSNa) according to a protocol, which is well established for larger clusters, such as for the transformation of $Au_{55}(PPh_3)_{12}Cl_6$ into $Au_{55}(Ph_2PC_6H_4SO_3Na)_{12}Cl_6$ [12]. However, physicochemical analysis revealed that this procedure, if applied to $[Au_9(PPh_3)_8](NO_3)_3$, leads to the formation of water-soluble Au_8 species [5, 9]. The loss of a single gold atom has already been observed in organic

solvents and was explained as an interconversion of [Au$_9$(PPh$_3$)$_8$](NO$_3$)$_3$ into [Au$_8$(PPh$_3$)$_8$](NO$_3$)$_2$ [13], which apparently prohibits the formation of the wanted water-soluble Au$_9$ cluster.

The crystallization and analysis by means of single-crystal X-ray diffraction (XRD) of phosphine gold clusters in general is challenging [14]. Especially in the case of water-soluble, TPPMSNa-stabilized clusters crystallization was not successful yet, presumably because of the flexibility of the ligands, the numerous charged groups and the large number of water molecules and counter ions involved (in general, each TPPMSNa is hydrated by two water molecules [12]).

In this paper we describe the synthesis and the XRD characterization of TPPMSNa-stabilized Au$_9$ clusters (**1**). Although a structure model of the whole cluster with atomic resolution could not be obtained, the core structure of **1** has been established. This led to the preliminary formula Na$_{(8-x)}$[Au$_9$(TPPMS)$_8$]Cl$_{(3-x)}$ · nH$_2$O ($0 \leq x \leq 3$, $n \approx 16$), which is corroborated by energy dispersive X-ray analysis (EDX) and ^{31}P{^{1}H} nuclear magnetic resonance spectroscopy (NMR). Furthermore the optical absorbance data are discussed against data of structurally related Au clusters.

Results and Discussion

Synthetic aspects and optical spectroscopy

Recently, we reported the synthesis of NIR light-absorbing 1.0 nm AuNPs with a mixed ligand shell of TPPMSNa and 3-mercaptopropionic acid (MPA) by mixing [Au(TPPMSNa)Cl] · H$_2$O one to one with MPA in ethanol followed by reduction with NaBH$_4$, within 17 h of stirring followed by purification by fractionated precipitation and column chromatography [15]. Polyacrylamide gel electrophoresis (PAGE) revealed three distinct fractions of AuNPs in the raw product after stirring (Fig. 1a).

Fraction 1 had intense brownish green color, while Fraction 2 appeared greyish, and the more separated Fraction 3 was of orange color. The individual regions of the gel were resected, separately diluted in water over night, filtered and examined *via* extinction spectroscopy (OES) (Fig. 1b). Fraction 1 reveals local absorbance maxima at 326, 373, 414, and 670 nm which are characteristic for the 1.0 nm TPPMSNa-MPA particles [15]. Fraction 2 shows less fine structure, and the spectrum can be considered as an exponential decay of the absorbance overlaid with two small features at 412 and 668 nm. The exponential component is characteristic for AuNPs between 1.2 and 2 nm and indicates 5d-6sp transitions of a developing band structure [16]. The two features are most probably caused by a small amount of particles from Fraction 1 smearing out into the less concentrated Fraction 2. In the spectrum of Fraction 3 only signals of overlapping bands with maxima below 500 nm, *i. e.* 312, 354, 382, and 443 nm, were observed. Such an absorbance pattern may reflect molecular phosphine-stabilized gold clusters smaller than 1 nm [6], and can serve as a fingerprint for [Au$_9$L$_8$]$^{3+}$ cluster cations, as will be shown below.
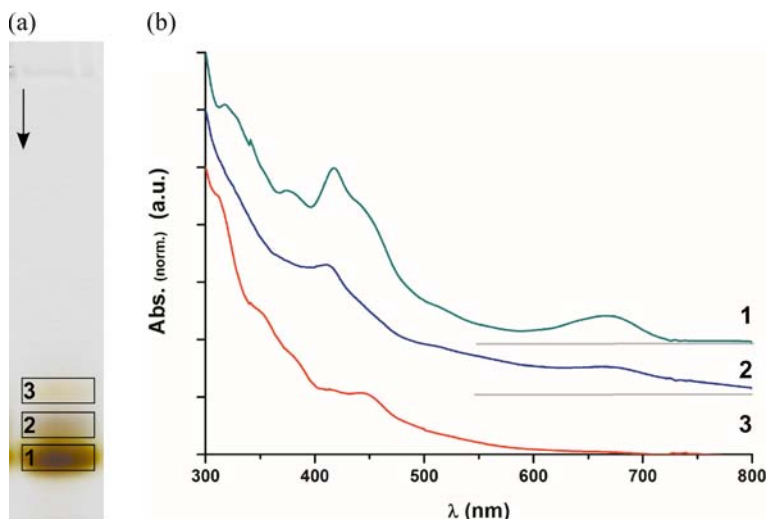

Fig. 1 (color online). (a) Photograph of a PAGE separation of AuNPs (arrow indicates the moving direction of the negatively charged particles towards the anode) and (b) the optical extinction spectra of each fraction. Fraction 1 is assigned to 1.0 nm AuNPs already introduced in ref. [15], fraction 2 is assigned to larger particles, whereas fraction 3 is expected to contain clusters of the general formula [Au$_9$L$_8$]$^{3+}$.
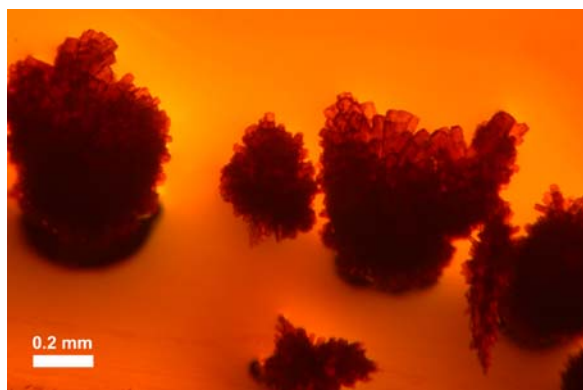
Fig. 2 (color online). Microscopic picture of the orange-red crystals of **1** formed during recrystallization.

Because the thiol mediates the solubility of [Au(TPPMSNa)Cl] · H_2O in ethanol, the synthesis was repeated with and without MPA (see Experimental Section) with shorter reaction times (5 h instead of 17 h) in order to decrease the formation of thermodynamically favored larger particles. By using fractionated precipitation [17] isolation of a fraction of small clusters, which eluate first, was achieved. Recrystallization was performed by slow diffusion of 2-propanol through the gas phase into an aqueous solution of the clusters. From both syntheses optically similar, orange-red crystals of **1** were obtained at the meniscus (Fig. 2).
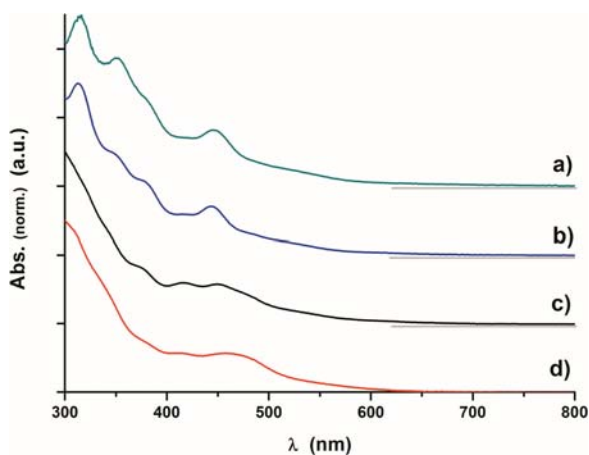

Fig. 3. Optical extinction spectra of dilute solutions of a) **1**, b) [Au₉(PPh₃)₈](NO₃)₃, c) TPPMSNa-stabilized Au₈ cluster, and d) [Au₈(PPh₃)₈](NO₃)₂. Spectra a) and c) were recorded in water, b) and d) in dichloromethane. Pure solvents were used for baseline correction.

Some crystals were collected, a dilute solution was analyzed *via* OES, and the spectrum was compared to data of structurally related Au clusters (Fig. 3).

The spectrum of **1** (Fig. 3a) shows local maxima at 312, 354, 382, and 443 nm as already observed in Fraction 3 of the electrophoresis. It nearly resembles the spectrum of [Au₉(PPh₃)₈](NO₃)₃ (Fig. 3), only the band at 354 nm is stronger in **1** which is probably caused by the influence of the ligand and/or the solvent. In addition, the pattern is significantly different from that of the Au₈ species [Au₈(PPh₃)₈](NO₃)₂ (Fig. 3c) and its TPPMSNa analog (Fig. 3d) which show absorbance maxima at 375 and 415 nm, as well as at 450 or 460 nm, respectively. Therefore, OES already indicates that **1** contains cluster cations of the type [Au₉L₈]³⁺.

Diffraction results on the core structure and elemental composition

Both syntheses (with and without MPA) of the TPPMSNa-stabilized cluster **1** only gave few crystals suitable for XRD. All their dimensions were less than 0.1 mm, and their diffraction was restricted to *ca.* 1.7 Å. In addition to the limited crystal size, the expected high degree of hydration of the cluster and, most likely, conformational disorder of the sulfonated phosphine contribute to the very low resolution of the diffraction pattern. Nevertheless, the experimental data provide very helpful information: Indexing of the diffraction pattern resulted in a tetragonal unit cell with a volume of 8810(4) Å³. When **1** is associated with a tentative chemical composition Na$_{(8-x)}$[Au₉(TPPMS)₈]Cl$_{(3-x)}$ · nH₂O ($0 \leq x \leq 3$, $n \approx 16$), a volume per formula unit between *ca.* 4100 and 4300 Å³ is predicted [18]. This tentative formula is further corroborated by EDX data, which confirm the presence of Na, Cl, and S besides P and Au. A unit cell content of $Z = 2$ can therefore be anticipated and is in good agreement with the expectation. Despite the low resolution of the diffraction data, space group determination and structure solution by the Patterson Method were successful: **1** crystallizes in space group $P4/n$; the central gold atom is located in Wyckoff position $2c$, in agreement with $Z = 2$ and the space filling criteria outlined above. Each asymmetric unit contains two gold atoms in general position, and hence as predicted from OES a Au₉ core of site symmetry 4 (point group C_4) is obtained. After refinement of this most basic
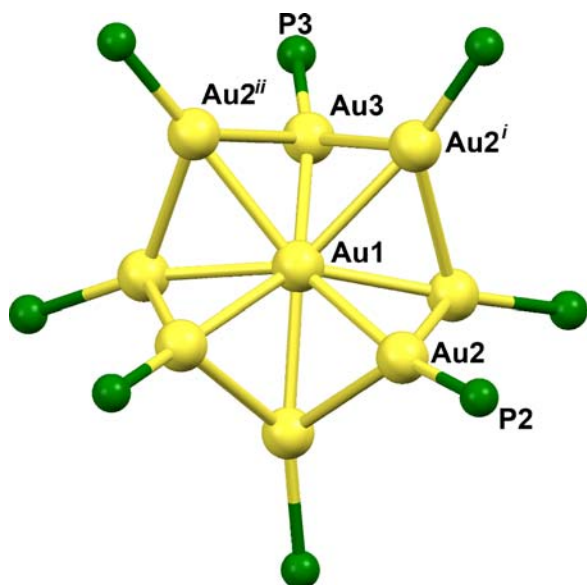
Fig. 4. Au_9 core structure of **1**. Symmetry operations: $i = 1/2 - y,\ x,\ z;\ ii = 1/2 - x,\ 1/2 - y,\ z$. The interatomic distances amount to Au1–Au2 2.681(12) Å, Au1–Au3 2.617(11) Å, Au2^i–Au3 2.776(13) Å, Au2^{ii}–Au3 2.802(13) Å, Au2–P2 2.12(8) Å, Au3–P3 2.30(8) Å.

structure model, two peripheric phosphorus atoms per asymmetric unit could be located. The core structure of **1** thus obtained is shown in Fig. 4. This crown structure has already been observed for other Au_9 clusters. $[Au_9(P(p\text{-}C_6H_4OMe)_3)_8](NO_3)_3$ can be crystallized in two skeletal isomers, the crown and the butterfly structure [10], whereas $[Au_9(PPh_3)_8](NO_3)_3$ prefers the butterfly conformation in the solid state [9]. The radial Au–Au distances (2.617(11) and 2.681(12) Å) are shorter then the peripheral distances (2.776(13) and 2.802(13) Å), and the Au–P distances amount to 2.12(8) and 2.30(8) Å. All distances are within the typical range for gold clusters [6, 19]. The stability of **1** can be explained by the formation of an ellipsoidal (2D) superatom complex which possesses an electron closure at 6 electrons within the binding cluster molecular orbitals [19]. Further details concerning the diffraction experiment are given in the Experimental Section.

Crystalline samples of **1** are very sensitive to dehydration: The single crystals had to be selected and manipulated under inert oil, and powder samples only gave a few broad maxima at low resolution. The first three intensity maxima could be associated with the

most intense lines from a simulated pattern based on the single crystal analysis.

$^{31}P\{^1H\}NMR$ spectroscopy

$^{31}P\{^1H\}NMR$ spectroscopy is suitable to compare signals of different small phosphine-stabilized clusters as well as monomeric gold complexes and free ligands [13]. Thus we recorded $^{31}P\{^1H\}NMR$ spectra of **1** in D_2O. The spectrum shows a singlet at 57.3 ppm, typical for gold clusters of this size. Neither signals of the monomeric complex $[Au(TPPMSNa)Cl] \cdot H_2O$ at 31.6 ppm nor of the free ligand TPPMSNa at -6.5 ppm could be observed.

Conclusion

The water-soluble, phosphine-stabilized $[Au_9]^{3+}$ cluster **1** has been synthesized and could be obtained as orange-red crystals. Characterization *via* OES, XRD, EDX, and $^{31}P\{^1H\}NMR$ experiments led to the preliminary formula $Na_{(8-x)}[Au_9(TPPMS)_8]Cl_{(3-x)} \cdot nH_2O$ $(0 \leq x \leq 3,\ n \approx 16)$ with the cluster core in crown conformation. According to the model of superatom complexes the cluster core $[Au_9L_8]^{3+}$ is expected to have an oblate elliptical (toroidal) closed electronic system. This is the first example where TPPMSNa-stabilized clusters form crystals which are suited to determine the positions of the gold and phosphorus atoms and thus the core structure of the cluster. The latter is of foremost importance to unravel the structure-property relationship within these materials and to elucidate mechanistic aspects within the molecularly precise synthesis of clusters. Synthetic efforts are ongoing to increase the yield of **1** in order to perform further physicochemical characterization and ultimately to test its cytotoxic potential.

Experimental Section

$[Au(TPPMSNa)Cl] \cdot H_2O$ was prepared in two steps by using protocols of Ahrland *et al.* [20] and Sanz *et al.* [21]. Protocols for $[Au_8(PPh_3)_8](NO_3)_2$ [13], TPPMSNa-stabilized Au_8 [5, 9] and $[Au_9(PPh_3)_8](NO_3)_3$ [9] are well described in the literature. Polyacrylamide gel electrophoresis (PAGE) suitable for the separation of molecular water-soluble gold clusters was performed according to Negishi *et al.* in a BioRad Mini-PROTEAN II [22]. $HAuCl_4 \cdot 3H_2O$ (Sigma-Aldrich), tetrahydrothiophene (Sigma-Aldrich), N,N'-methylenebis(acrylamide)

(Sigma-Aldrich), acrylamide (Sigma-Aldrich), (*N*,*N*,*N'*,*N'*)-tetramethylenediamine (Sigma-Aldrich), Trizma® Base (Sigma-Aldrich), TRIS glycine buffer solution (Fluka), ammonium peroxodisulfate (Sigma-Aldrich), ethanol (Grüssing), 3-mercaptopropionic acid (MPA, Sigma-Aldrich), NaBH$_4$ (Sigma-Aldrich), toluene (Fischer Scientific), dichloromethane (VWR), and 2-propanol (Fischer Scientific) were used as received. Water was taken from an ELGA Purelab Plus. OES was performed in a Jasco V-630 and NMR spectroscopy in a Bruker Avant II 400 instrument. 85 % phosphoric acid was used as external ^{31}P NMR standard. EDX measurements were performed in a Leo/Zeiss FE-SEM Supra 35 VP instrument equipped with an Oxford INCA Energy 200 (SiLi crystal, 133 eV, 10 mm^2).

(Na)$_{8-x}$[Au$_9$(TPPMS)$_8$](Cl)$_{3-x}$ · n(H$_2$O) with MPA

Synthesis was performed in analogy to [15], with a shorter reaction time. 433.5 mg (0.7 mmol) [Au(TPPMSNa)Cl] · H$_2$O was suspended in 40 mL of ethanol, and 61.2 µL (0.7 mmol) MPA was added while gently mixing the suspension. After dissolution of the solid a freshly prepared solution of 7.6 mg (0.2 mmol) NaBH$_4$ in 6.5 mL ethanol was added dropwise to the clear solution. After stirring for 5 h the brown solution was filtered, and the solvent was removed.

Then the solid was dissolved in 1.730 mL water and precipitation was induced by the addition of 19.5 mL 2-propanol. The precipitate was collected by centrifugation, and the steps of dissolution, precipitation and centrifugation were repeated. The remaining red solution was set aside and a precipitate formed within one day. Few orange-red crystals of the product formed during the slow diffusion of 2-propanol *via* the gas phase into a solution of the precipitate in water-2-propanol (1 : 5).

(Na)$_{8-x}$[Au$_9$(TPPMS)$_8$](Cl)$_{3-x}$ · n(H$_2$O) without MPA

452 mg (0.72 mmol) [Au(TPPMSNa)Cl] · H$_2$O were suspended in 44 mL of ethanol and stirred at room temperature. A freshly prepared solution of 8 mg (0.21 mmol) NaBH$_4$ in 7 mL of ethanol was added dropwise to the solution. After stirring for 5 h the brown solution was filtered and the solvent was removed.

The solid was dissolved in 10 mL of water and precipitated by the addition of acetone, centrifuged and again dissolved in water. This process was repeated three times. The remaining solid was dried under high vacuum, and 30 mg of the raw product were dissolved in 300 µL of water. Slow diffusion of 2-propanol induced the formation of orange-red crystals.

X-Ray structure determination

Single-crystal X-ray diffraction for **1**: Data were collected at 100 K on a Bruker D8 goniometer equipped with an APEX CCD detector using MoK_α radiation ($\lambda = 0.71073$ Å). The radiation source was an INCOATEC I-µS microsource, and an Oxford Cryosystems 700 controller was used to ensure temperature. The sample was a red plate-like crystal with approximate dimensions $0.05 \times 0.04 \times 0.07$ mm^3. Crystal data: C$_{144}$H$_{144}$Au$_9$Cl$_3$Na$_8$O$_{40}$P$_8$S$_8$, $M_r = 5081.80$, tetragonal space group $P4/n$, $a = 25.188(8)$, $c = 13.886(5)$ Å, $V = 8810(4)$ Å^3, $Z = 2$, $d_{\mathrm{calcd.}} = 1.92$ Mg cm^{-3}, $\mu = 7.8$ mm^{-1}, $F_{000} = 4852$. The SAINT software [23] was used for integration and SADABS [24] for multi-scan absorption correction. Our data collection originally extended to a resolution of 0.9 Å, comprising 15828 reflections; however, less than 50 % of the measured intensities at a resolution of 1.7 Å fulfilled the condition $I > 2 \sigma(I)$. Data were truncated at 1.37 Å (corresponding to a diffraction range $2\theta \leq 30°$ for MoK_α); at this resolution, 1680 independent reflections remained, and an average ratio $I/\sigma(I)$ of 2.5 was achieved. In the model for the core structure, only the Au with anisotropic and the P atoms with isotropic displacement parameters were considered. The crystal used in the diffraction experiment turned out to be a merohedral twin, with twin lattice symmetry $4/mmm$; a small contribution of a second domain (volume fraction 16.7(10) %) was taken into account. After refinement of the core model, the maximum residual electron density amounted to 3.9 e Å^{-3} in the vicinity of an Au atom; in line with this fact, our attempts to assign additional electron density to ordered C atoms of the phosphine ligand or to the substituting sulfonyl groups did not result in stable refinements. The core model comprised 31 parameters; it converged with conventional agreement factors $R = 0.2791$ for all 1680, $R = 0.2453$ for 1249 observed data with $I > 2 \sigma(I)$ and $R_{\mathrm{free}} = 0.2879$ [25] for a reference set of 88 data.

The powder XRD was conducted in the transmission mode on thin films by using a Huber diffractometer G670 with Cu$K_{\alpha 1}$ radiation ($\lambda = 1.5418$ Å).

CCDC 932511 contains the supplementary crystallographic data for this paper. These data can be obtained free of charge from The Cambridge Crystallographic Data Centre *via* www.ccdc.cam.ac.uk/data_request/cif.

[1] G. Schmid, *Chem. Rev.* **1992**, *92*, 1709 – 1727.

[2] M.-C. Daniel, D. Astruc, *Chem. Rev.* **2004**, *104*, 293 – 346.

[3] R. W. Murray, *Chem. Rev.* **2008**, *108*, 2688 – 2720.

[4] M. Tsoli, H. Kuhn, W. Brandau, H. Esche, G. Schmid, *Small* **2005**, *1*, 841 – 844.

[5] Y. Pan, S. Neuss, A. Leifert, M. Fischler, F. Wen, U. Simon, G. Schmid, W. Brandau, W. Jahnen-Dechent, *Small* **2007**, *3*, 1941 – 1949.

[6] K. P. Hall, D. M. P. Mingos in *Progress in Inorganic Chemistry* (Ed.: S. J. Lippard), John Wiley & Sons, Inc., **2007**, pp. 237 – 325.

[7] L. Malatesta, L. Naldini, G. Simonetta, F. Cariati, *Coord. Chem. Rev.* **1966**, *1*, 255 – 262.

[8] G. Schmid, R. Pfeil, R. Boese, F. Bandermann, S. Meyer, G. H. M. Calis, J. W. A. van der Velden, *Chem. Ber.* **1981**, *114*, 3634 – 3642.

[9] F. Wen, U. Englert, B. Gutrath, U. Simon, *Eur. J. Inorg. Chem.* **2008**, 106 – 111.

[10] C. E. Briant, K. P. Hall, D. M. P. Mingos, *J. Chem. Soc., Chem. Commun.* **1984**, 290 – 291.

[11] M. Schulz-Dobrick, M. Jansen, *Eur. J. Inorg. Chem.* **2006**, 4498 – 4502.

[12] G. Schmid, N. Klein, L. Korste, U. Kreibig, D. Schönauer, *Polyhedron* **1988**, *7*, 605 – 608.

[13] J. W. A. Van der Velden, J. J. Bour, W. P. Bosman, J. H. Noordik, *Inorg. Chem.* **1983**, *22*, 1913 – 1918.

[14] J. M. M. Smits, P. T. Beurskens, J. J. Steggerda, *J. Chem. Crystallogr.* **1983**, *13*, 381 – 384.

[15] B. S. Gutrath, M. F. Beckmann, A. Buchkremer, T. Eckert, J. Timper, A. Leifert, W. Richtering, G. Schmitz, U. Simon, *Nanotechnology* **2012**, *23*, 225707.

[16] R. E. Benfield, A. P. Maydwell, J. M. van Ruitenbeek, D. A. van Leeuwen, *Z. Phys. D* **1993**, *26*, 4 – 7.

[17] G. A. Ozin, A. C. Arsenault, L. Cademartiri, *Nanochemistry: A Chemical Approach to Nanomaterials*, RSC Publishing, London **2008**.

[18] D. Hofmann, *Acta Crystallogr. B* **2002**, *58*, 489 – 493.

[19] B. S. Gutrath, I. M. Oppel, O. Presly, I. Beljakov, V. Meded, W. Wenzel, U. Simon, *Angew. Chem. Int. Ed.* **2013**, *52*, 3529 – 3532.

[20] S. Ahrland, K. Dreisch, B. Norén, Å. Oskarsson, *Mater. Chem. Phys.* **1993**, *35*, 281 – 289.

[21] S. Sanz, L. A. Jones, F. Mohr, M. Laguna, *Organometallics* **2007**, *26*, 952 – 957.

[22] Y. Negishi, K. Nobusada, T. Tsukuda, *J. Am. Chem. Soc.* **2005**, *127*, 5261 – 5270.

[23] Saint (version 6.02), Program for Reduction of Data Collected on a Bruker CCD Area Detector Diffractometer, Bruker Analytical X-ray Instruments Inc., Madison, Wisconsin (USA) **1999**.

[24] G. M. Sheldrick, Sadabs (version 2004/1), Program for Empirical Absorption Correction of Area Detector Data, University of Göttingen, Göttingen (Germany) and Bruker Analytical X-ray Instruments Inc., Madison, Wisconsin (USA) **2004**.

[25] A. T. Brünger, *Nature* **1992**, *355*, 472 – 475.